JOURNAL OF GEOPHYSICAL RESEARCH, VOL. 99, NO. C12, PAGES 24,517–24,526, DECEMBER 15, 1994

Calibration of the TOPEX altimeter using a GPS buoy

George H. Born, Michael E. Parke, Penina Axelrad, Kenneth L. Gold, James Johnson, Kevin W. Key, and Daniel G. Kubitschek

Colorado Center for Astrodynamics Research, University of Colorado at Boulder

Edward J. Christensen

Jet Propulsion Laboratory, California Institute of Technology, Pasadena

Abstract. The use of a spar buoy equipped with a Global Positioning System (GPS) antenna to calibrate the height measurement of the TOPEX radar altimeter is described. In order to determine the height of the GPS antenna phase center above the ocean surface, the buoy was also equipped with instrumentation to measure the instantaneous location of the waterline, and tilt of the buoy from vertical. The experiment was conducted off the California coast near the Texaco offshore oil platform, Harvest, during cycle 34 of the TOPEX/POSEIDON observational period. GPS solutions were computed for the buoy position using two different software packages, K&RS and GIPSY-OASIS II. These solutions were combined with estimates of the waterline location on the buoy to yield the height of the ocean surface. The ocean surface height in an absolute coordinate system combined with knowledge of the spacecraft height from tracking data provides a computed altimeter range measurement. By comparing this computed value to the actual altimeter measurement, the altimeter bias can be calibrated. The altimeter height bias obtained with the buoy using K&RS was -14.6±4 cm, while with GIPSY-OASIS II it was -13.1±4 cm. These are 0.1 cm and 1.6 cm different from the -14.7±4 cm result obtained for this overflight with the tide gauge instruments located on Platform Harvest.

Introduction

During the evening of October 17, 1993 PST, the morning of October 18, UTC, the University of Colorado in cooperation with the Jet Propulsion Laboratory deployed a spar buoy equipped with a TurboRogue Global Positioning System (GPS) antenna under the ground track of the TOPEX/POSEIDON (T/P) spacecraft. The antenna was connected via a cable to a GPS receiver on a nearby boat. The buoy was deployed off the coast of California adjacent to the offshore Texaco platform, Harvest (see Figure 1). The Harvest Platform is the NASA calibration site for T/P [*Morris et al.,* 1995]. The objective of this experiment was to investigate an alternative calibration technique to determine the range bias in the TOPEX radar altimeter using the GPS buoy, GPS receivers located at Vandenburg Air Force Base and on the Harvest Platform, and the tracking systems on board the spacecraft. These systems are a GPS receiver, a laser retroreflector, and the French Doppler system, Doppler Orbitography and Radiopositioning Integrated by Satellite (DORIS).

Paper number 94JC00920.
0148-0227/94/94JC-00920$05.00

Given the altitude of the spacecraft determined from these tracking systems and the height of local sea level as determined by a differential GPS solution using the buoy and a fiducial GPS receiver, one can compare the altimeter range measurement to the calculated range and determine the bias. We estimate that the GPS buoy can determine sea level as a function of time to ±2.2 cm based on an error budget of 1 cm for the position of the L3 phase center relative to the waterline using instruments attached to the buoy and 2 cm for the GPS solution of the phase center location in absolute coordinates. Current knowledge of the T/P orbit height is 3.5 cm, 1σ, based on laser and DORIS data [*Tapley et al.,* this issue] and better than 3 cm, 1σ, based on GPS data [*Bertiger et al.,* this issue]. This means that the altimeter range bias can be determined to an RMS accuracy of about 4.1 cm with laser and DORIS orbits and 3.7 cm or better with GPS orbits on any given pass. Because of operational constraints, GPS orbits are not always available; however, they were for this experiment.

There are several reasons for requiring periodic calibration of the altimeter height measurement. Any drift in the range bias results in an apparent rise or fall in global sea level. Furthermore, drifts in the range bias will corrupt basin-scale circulation patterns deduced from altimeter data. The increased accuracy to which the radial component of the T/P orbit is being deter-

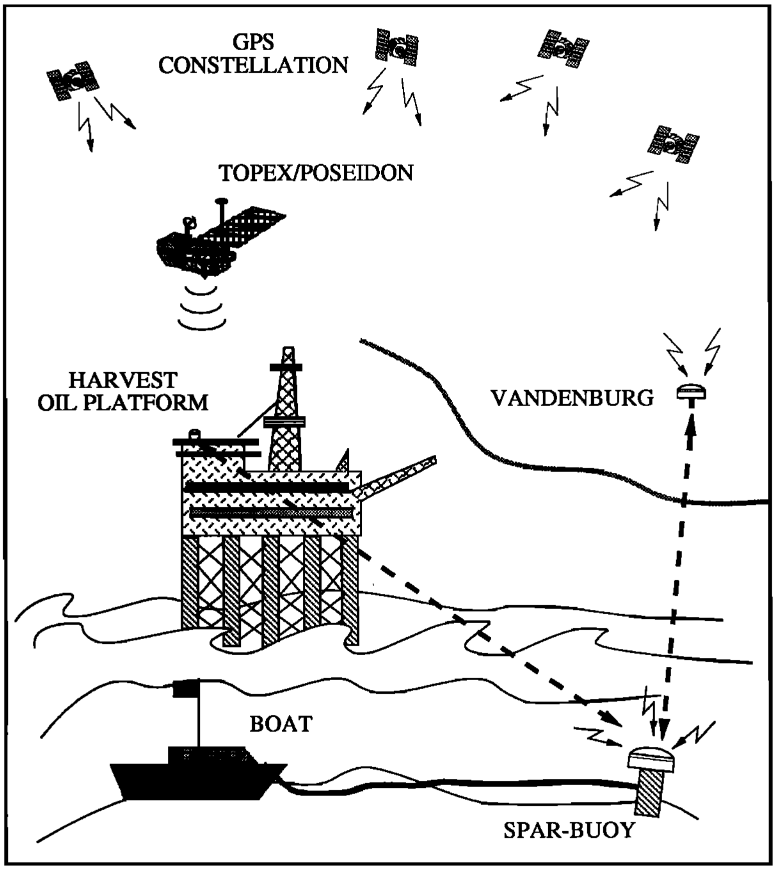

Figure 1. Experiment configuration overview.

mined will allow basin-scale circulation patterns to be measured to unprecedented accuracy, but only if the range bias is understood. Thus it becomes increasingly important to ensure the accuracy of the altimeter range measurement. Knowledge of the bias itself is important, even if there is no drift, in order to tie the elevation of mean sea level from T/P to that of future altimetric missions such as the follow-on missions for T/P, Geosat, and ERS 1. If the fidelity of the absolute height measurements from these missions cannot be maintained, there is little hope of monitoring the long-term rise and fall of sea level to useful accuracy.

Our first experiments with a GPS-equipped buoy took place off the Scripps pier at La Jolla, California in December 1989 [*Rocken et al.,* 1990]. This buoy was basically a waverider (designed to ride up and down with the waves). Our first spar buoy (designed to have as little vertical motion as possible) was deployed adjacent to the Harvest Platform in August of 1990 in order to gain experience with the buoy and to provide an opportunity to test the operational procedure for deploying the buoy and gathering data after the launch of T/P [*Kelecy et al.,* 1992]. In addition, the spar buoy and a GPS-equipped waverider buoy were deployed in November 1991, under the ground track of the ERS 1 satellite. This spacecraft also carries an altimeter, and the objectives of this experiment were to test the two buoy configurations and to calibrate the ERS 1 altimeter range bias [*Kelecy et al.,* 1994].

Experiment Description

The spar buoy used in this experiment is sketched in Figure 2 and is described in detail by *Kelecy et al.* [1994]. Table 1 presents the locations of the instruments on the buoy. Overall, the buoy is about 13 m long with a radome at the top to house the GPS antenna. Two Paroscientific depth sensors are located on the buoy, as shown in Figure 2, in order to help determine the location of the waterline during the experiment and to measure any tilt of the buoy. In addition, a MagneRule PLUS was located on the buoy in order to provide an independent measure of the distance between the waterline and the GPS antenna phase center. The MagneRule PLUS consists of a stainless steel rod with a float that can slide along the rod. With calibration, the instrument is capable of reporting the position of the float with an accuracy of about 1 mm over the range of its 2.44 m scale. The depth sensors each consist of a pressure transducer and temperature sensor. The

Table 1. Buoy Instrument Locations

Interval	Distance, m
L3 phase center to base of radome	0.088
MagneRule zero to base of radome	0.480
Depth sensor 1 to base of radome	4.810
Depth sensor 3 to base of radome	7.611

pressure measurements are internally compensated for temperature dependence. The depth sensors are calibrated side by side with a portable standard, both in the air and with the depth sensors in a known amount of water. The air calibration establishes the bias in the measurements while the water calibration establishes the effective measurement point on each depth sensor. The resulting accuracy of the depth sensors is about 1 cm.

The buoy design used in this experiment was developed in order to minimize vertical motion of the radome at the top of the spar. There are two components to this motion: vertical buoy motion in response to gravity waves and tilting of the buoy both due to response to waves and due to tension on the tether. Tilting of the buoy contributes to the vertical location of the radome as the cosine of the angle of the buoy from vertical. When the buoy is allowed to float freely (requiring active maneuvering by the pilot of the boat) there is little or no mean tilt. Otherwise there is both a mean tilt and a change in the location of waterline on the buoy. The relative importance of each depends on the location at which the tether is attached to the buoy. The difficulty of maintaining slack on the buoy tether is one of the motivations for developing an autonomous buoy as described later. Tilting of the buoy in response to waves is minimized by the design of the buoy and should have a negligible impact. The instrumentation on the buoy is designed to provide both a redundant measure of the waterline position and the ability to monitor the mean tilt of the buoy. By doing this we can avoid the complexities of a waterline calibration under difficult at sea conditions and errors caused by changing tensions on the buoy tether.

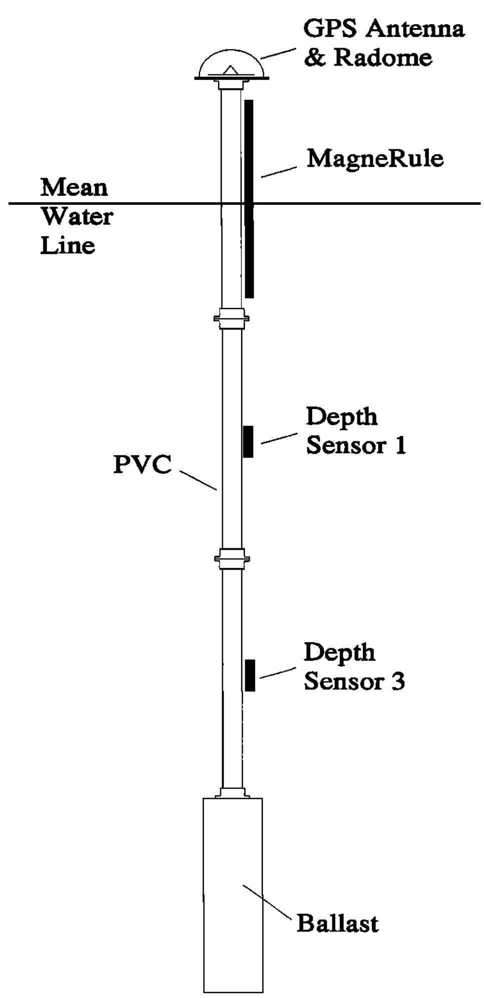

Figure 2. Schematic of the spar buoy design.

Several hours prior to the T/P spacecraft overflight, the buoy was deployed from Platform Harvest and towed by boat a short distance from the platform to await the arrival of the spacecraft. The TurboRogue receiver was carried on the boat and connected via cable to the antenna in the radome of the buoy. After deployment, over 1 hour of high rate (1/s) GPS data were taken, centered on the overflight time of the spacecraft (August 18, 1993, 0050:29.3081 UTC). Only about 50 min of MagneRule and depth sensor data were taken, however, due to delays in starting the instruments. Data also were taken on the platform in both high-rate (1/s) and low-rate (1/30 s) modes using two Turbo Rogue receivers hooked to the same antenna. In addition, high-rate data were taken by a Rogue receiver at a fiducial site at Vandenburg Air Force Base.

All tracking systems were operational around the time of the overflight, insuring quality orbit solutions. Laser tracking of the T/P spacecraft was obtained from Mazatlan, Quincy, and Monument Peak. In addition, the spacecraft was tracked by GPS and the global complement of DORIS stations. MagneRule data were collected every 0.5 s and depth sensor data were collected every second. The MagneRule directly measures the position of the waterline on the buoy, while the depth sensors measure a combination of air pressure, static water pressure, and wave pressure effects.

Two National Oceanic and Atmospheric Administration (NOAA) tide gauges located on Platform Harvest were in operation during the overflight [*Gill et al.,* 1995] thus allowing a comparison of the tide gauge sea level with that determined by the buoy. These are part of the NOAA Next Generation Water Level Measurement System. The primary gauge was an acoustic system using round trip travel times to measure sea level (which is the standard tide station configuration now being implemented by NOAA). The secondary system for water level measurement was a nitrogen-driven bubbler system implemented with a Paroscientific depth sensor. These will be referred to as the NOAA acoustic and NOAA Digibub systems for the rest of this paper.

GPS Solutions

Two GPS software packages were used in this study: Kinematic and Rapid Static (K&RS) developed by *Mader* [1986] at NOAA and GIPSY-OASIS II (GOA II) developed at the Jet Propulsion Laboratory (JPL) [*Lichten and Border,* 1987]. K&RS was developed specifically for high-precision kinematic positioning such as the application presented here. GOA II was developed for more general applications such as high-precision geodesy (using global-scale networks) and GPS-based orbit determination for low Earth orbiters. In both cases L3 phase center solutions were generated by appropriate linear combination of the carrier phase measurements at the L1 (1575.42 MHz) and L2 (1227.60 MHz) frequencies to produce an "ionosphere free" solution. The following two paragraphs give brief summaries of the two techniques as they were applied to the GPS buoy problem.

K&RS produces an independent geometric buoy position for each epoch using double difference carrier phase measurements to eliminate clock errors. Reference locations and atmospheric models are treated as absolutes. To estimate tropospheric corrections, K&RS uses a modified Marini model [*Mader*, 1986]. Double difference carrier ambiguities are resolved as fixed integers. The K&RS solution presented here was carried out over the 11-km baseline between the GPS location at Vandenburg and the GPS buoy using National Geodetic Survey precise orbits for the GPS satellites [*Schenewerk et al.*, 1993]. Local meteorological conditions were measured at the platform [*Gill et al.*, 1995] and at Vandenberg using radiosonde data to provide input to the modified Marini model. Conditions at the platform were extrapolated to the buoy location assuming a dry adiabatic lapse rate for temperature and a standard pressure gradient. Relative humidity was adjusted by assuming that the water vapor pressure was constant. At the time of overflight, the buoy was separated by about 1.5 km horizontally and 30 m vertically from the location on Platform Harvest where the meteorological data were taken. Meteorological measurements were necessary both at Vandenberg and Harvest because of differences in the atmosphere over the sites even though they were only about 11 km apart. This may have been due either to the fact that the Vandenberg receiver was inland or that an atmospheric front was in the vicinity at the time of the overflight. Extrapolating meterological measurements from the Harvest Platform to Vandenberg would have resulted in changes in the K&RS GPS buoy position of greater than 2 cm.

GOA II uses a Kalman-type filter to estimate the buoy position, as well as other parameters, as a function of time. The GOA II solution presented here involves GPS data from Vandenburg, Platform Harvest, the T/P satellite, and the the GPS buoy. GPS satellite orbits were obtained from the JPL daily analysis. The locations of Vandenburg and Platform Harvest were treated as fiducial sites with coordinate uncertainties of 0.001 m. The buoy position was modeled as a random walk process with a dynamic uncertainty of 5 $m/\sqrt{s}$. The clock errors for Platform Harvest and the buoy (relative to the Vandenburg clock) were each modeled as a white random process. GOA II uses the Lanyi model [*Lanyi*, 1984] as a nominal starting point for estimating the total tropospheric delay. In general, GOA II uses one or more parameters in the filter to estimate a residual tropospheric delay at each station, which includes both the total wet tropospheric delay and any error in the Lanyi dry delay model. For this experiment, the buoy tropospheric parameter was treated as a bias with an uncertainty of 0.5 m. This was necessary because the GPS buoy experiences significant vertical motions, and the observations were limited to only five satellites over a relatively short data arc (less than 60 min). More observations would be required to reliably separate vertical motions from changes in the tropospheric delay. Furthermore, because the data in this experiment were also limited in spatial separation of the stations (less than 100 km), only a single tropospheric residual for all three stations was estimated. The carrier phase bias for each tracked satellite was similarly estimated as a bias in the filter. The International Terrestrial Reference Frame of 1992 [*International Earth Rotation Service*, 1993] was used to provide coordinates corrected for plate motion to August 1993, for the Vandenburg and Harvest GPS markers.

Results

Figure 3 shows the horizontal track of the buoy relative to the Harvest Platform from GPS measurements. Platform Harvest, denoted by H in the figure, is located at 34.470923 N and 120.685845 W [*Christensen et al.*, this issue]. During data aquisition the buoy traversed approximately 1.6 km in a southeasterly direction. Slack was maintained in the line between the buoy and the boat in order to allow the buoy to float freely, thereby minimizing vertical offsets and tilting of the buoy.

The raw and filtered history of the L3 phase center of the GPS antenna from the K&RS solution is shown relative to the T/P reference ellipsoid in Figure 4. The T/P ellipsoid has a semimajor axis of 6378.1363 km and a flattening of 1/298.257. The GOA II solution is not shown because it is virtually identical at the scale presented. The raw phase solutions can be used to infer the local wave height, assuming a time history of the waterline on the buoy is available from an instrument such as the MagneRule. The slope observed in the filtered result is due predominantly to tides.

Figure 5 shows the raw and filtered data obtained from the MagneRule and the two Paroscientific depth sensors. The MagneRule data have been converted from volts to meters and are referenced to the top position of the float (see Table 1). The depth sensor measurements are in units of meters of fresh water and include atmospheric pressure as well as static and dynamic pressures due to the water column. The changes in the waterline relative to the buoy are a combination of wave motions and buoy motions. The effect of buoy motion on each of the sensors will be the same while the pressure effects due to wave motion will decrease with depth. Note the attenuation of the wave signals in the depth sensor data.

The data from the two depth sensors were used to compute tilt of the buoy during the experiment so that the GPS antenna phase center height above the reference ellipsoid could be corrected. The pressure difference histories of the two depth sensors indicated that

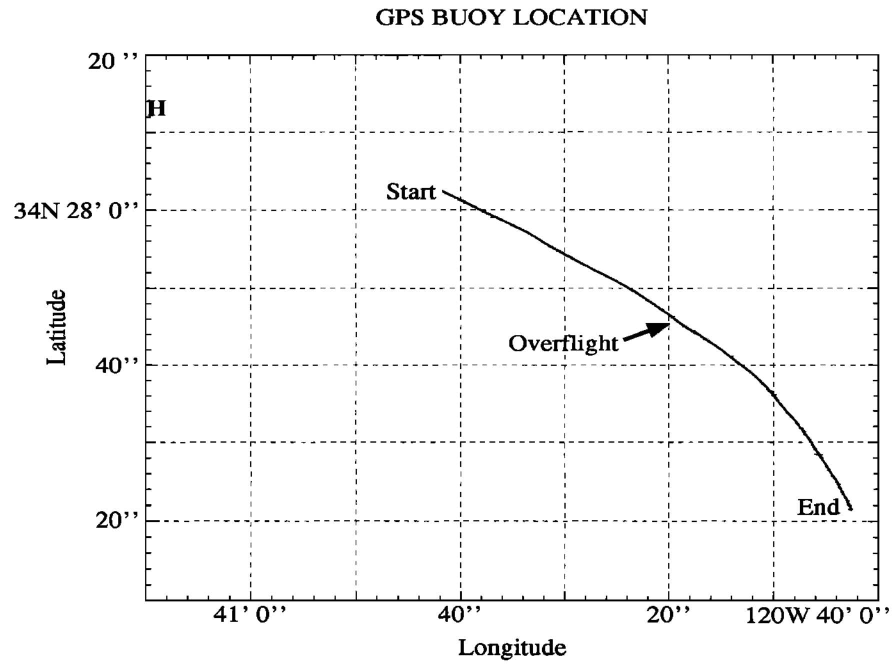

Figure 3. GPS buoy locations during the experiment based on the K&RS solution. The location of Platform Harvest is indicated by the H in the upper left corner.

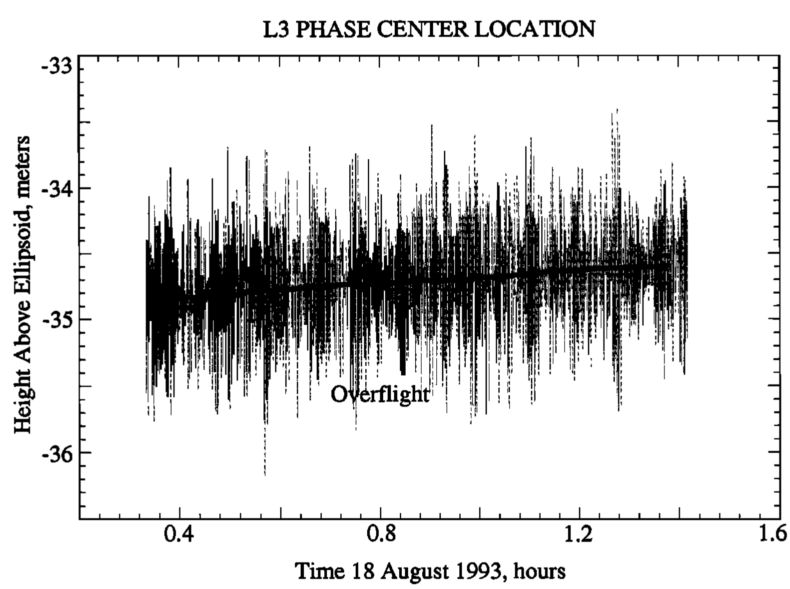

Figure 4. Location of the buoy-GPS antenna L3 phase center based on the K&RS solution. The GOA II solution is essentially the same at these scales.

at the overflight time, the height of the GPS antenna phase center was in error by less than 2 mm due to buoy tilt, suggesting that our attempts to allow the buoy to float freely were successful.

Sea level was determined by combining the GPS data, indicating the position of the L3 phase center of the GPS antenna, with data indicating the position of the waterline. Here two independent measures of the waterline are possible. Since the positions of the waterline from the two depth sensors agreed to better than 1 cm with the location of the waterline from the MagneRule and use of the MagneRule data allows direct determination of sea state, only the sea level from the MagneRule is presented here. Figure 6 shows the raw and filtered height of sea level above the T/P reference ellipsoid as determined from a combination of the L3 phase center

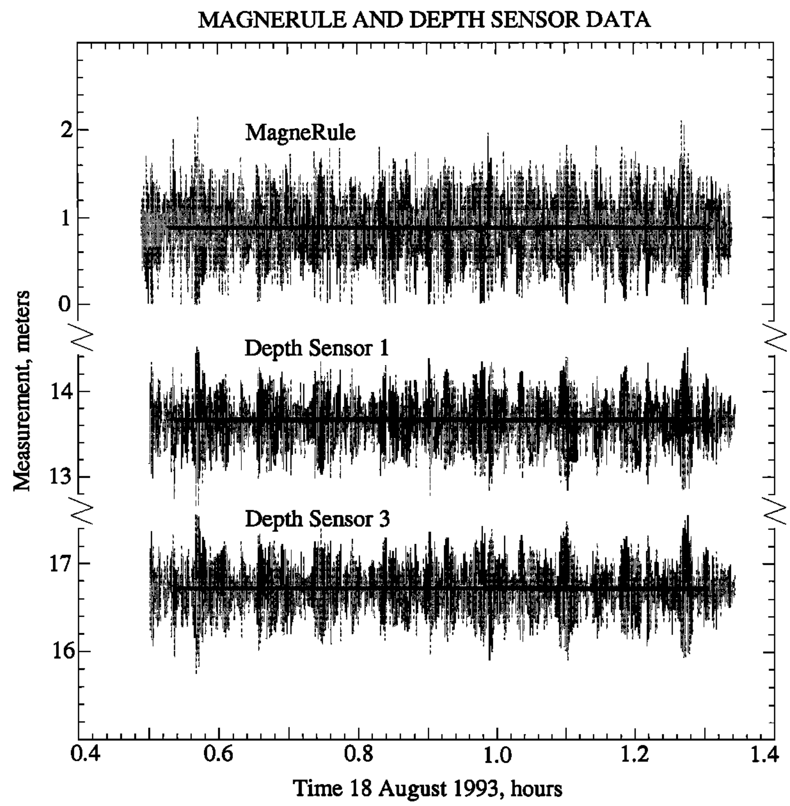

Figure 5. Raw and filtered MagneRule and depth sensor data. The Magnerule data have been converted from volts to meters (measured downward) and are referenced to the top position of the float. The depth sensor measurements are in units of meters of fresh water and include atmospheric pressure as well as static and dynamic pressures due to the water column.

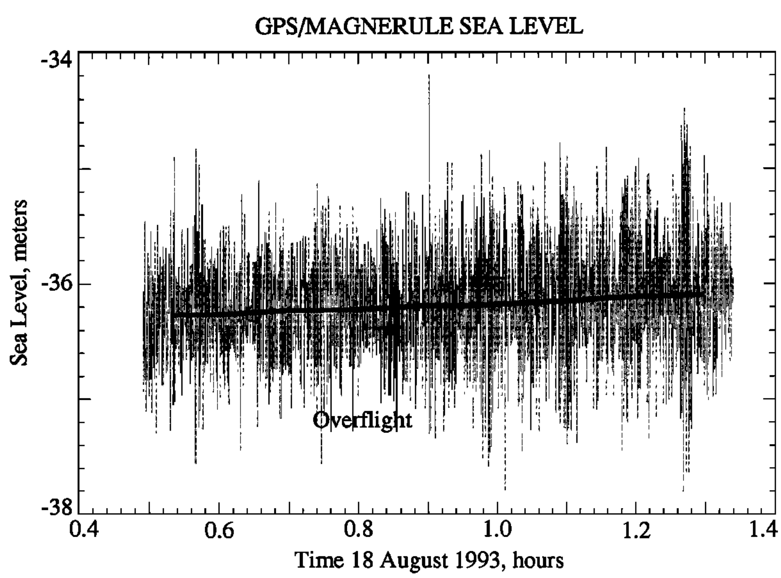

Figure 6. Sea level from the K&RS GPS solution combined with MagneRule data. Results based on the GOA II solution are essentially the same at these scales.

heights from the K&RS solution and the MagneRule waterline information in Figure 5.

The GPS buoy and Platform Harvest were not precisely colocated, and so a correction needs to be made for the expected difference in mean sea level between the platform and buoy. Based on Rapp's mean altimetric surface [*Bašić and Rapp*, 1992], the difference in mean sea level between the platform and the buoy was

-0.008 m at the start of measurements, -0.010 m at the time of overflight, and -0.000 m at the end of the measurements. Figure 7 compares the height of sea level above the reference ellipsoid determined from the two NOAA tide gauges located on Platform Harvest with the filtered GPS results from both K&RS and GOA II as adjusted for the Rapp gradient. The tide gauge measurements were converted to absolute sea level using the results of a survey between the instruments and a GPS receiver near the top of the platform [*Gill et al.*, 1995] and a GPS determined location for the receiver [*Christensen et al.*, this issue]. At the time of overflight, platform sea level with respect to the T/P ellipsoid from K&RS was -36.162 m, from GOA II was -36.147 m, from the NOAA acoustic tide gauge -36.163 m, and from the NOAA Digibub tide gauge -36.170 m. Table 2 provides statistical comparisons over the length of the pass. The two GPS solutions had a mean difference of 0.9 cm and a standard deviation of 1.2 cm over this interval. It is encouraging that the mean difference between the GPS solutions and the primary tide gauge measurement is the same or less than the standard deviation for both solutions.

Figure 8 is a panel of several examples of gravity wave spectra determined from the raw GPS/MagneRule sea level shown in Figure 6. The spectra show two distinct wave trains moving through the area with periods of about 8 and 14 s. Beginning about the time of the overflight, there is an increase in the power of the higher-frequency wave train corresponding to a frontal passage. This was observed by the boat crew as an increase in wind speed and wave height.

Spectra of the wave field were determined using fast Fourier transform (FFT) techniques from 256 1-s points with each set of data overlapping the previous set by 128 points. Before the FFT was applied, the mean and a linear trend were removed and a cosine taper applied to 10% of the data at each end. A Parzen window with a cutoff point of 100 lags was used to smooth the spectral estimates [see *Bendat and Piersol*, 1971]. $H_{1/3}$ estimates shown in Figure 9 were calculated as 4 times the standard deviation of the wave field for each of the spectral data sets. The period of increasing wave height associated with the frontal passage is clearly indicated. The altimeter recorded a value of 1.5 m for $H_{1/3}$ at the overflight time compared with 1.65 m derived from the buoy data. The history of $H_{1/3}$ measurements recorded by the altimeter indicates that it also crossed this front in the vicinity of the platform. The presence of a front near the point measurement site of the platform makes it difficult to compare the point measurement with the spatially averaged altimeter measurement. The probable cause for the buoy yielding a higher value of $H_{1/3}$ than the altimeter is that the front had just passed the platform about 2 min before the altimeter arrived. Hence the altimeter footprint contained larger waves behind the front and smaller waves ahead of the front. The spatial average of these tended to yield a lower number for $H_{1/3}$ than the buoy measured.

This experiment was performed to demonstrate the usefulness of a GPS buoy for calibrating altimetric satellites. For this reason the GPS buoy measurements were taken coincident with the normal calibration measurements. *Christensen et al.* [this issue] have determined the bias in the TOPEX altimeter range to be -14.7±4 cm for this overflight. The bias was calculated by combining the ocean surface height in an absolute coordinate system with knowledge of the spacecraft height from tracking data to provide a computed altimeter range measurement. By comparing this computed value to the actual altimeter measurement, the altimeter bias was found. Converting the tide gauge measurements to

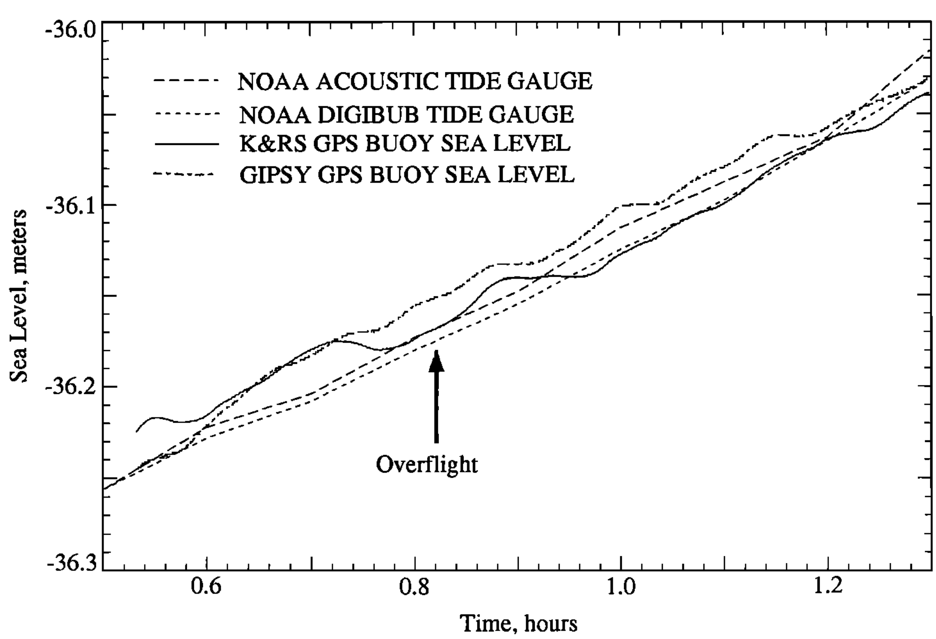

Figure 7. GPS/MagneRule sea level and tide gauge comparison. The tide gauge measurements have been converted to absolute sea level.

Table 2. GPS versus Tide Gauge Comparisons

Comparison	Mean, m	σ,* m
K&RS versus NOAA acoustic	0.000	0.013
GOA II versus NOAA acoustic	0.009	0.009
K&RS versus NOAA Digibub	0.007	0.011
GOA II versus NOAA Digibub	0.016	0.008

*Standard Deviation

an absolute reference frame requires that there be an accurate survey performed between the tide gauges and a known reference (in this case a GPS receiver near the helicopter pad on the platform). The only difference in closure using a GPS buoy is that the GPS buoy is used to provide absolute sea level instead of a tide gauge, survey, and reference marker. Here we are substituting the GPS buoy sea levels based on K&RS and GOA II for the NOAA acoustic tide gauge values used by Christensen et al. and conclude that the altimeter range bias for this overflight is -14.6±4 cm for the K&RS solution and -13.1±4 cm for the GOA II solution.

Discussion

The major advantage of the buoy approach over a fixed platform is that the calibration can be carried out anywhere in the world in the vicinity of any one of hundreds of fiducial GPS receiver sites. We are currently developing a low-cost autonomous buoy designed for a variety of offshore science experiments including satellite altimeter calibration and measurement of ocean currents. The mechanical design of the buoy is similar to the spar used in the experiments described here. The basic buoy equipment will include an L band choke ring antenna, a GPS receiver, a MagneRule, a single-board computer, a UHF antenna and radio modem, and two pressure transducers. A data collection and differential GPS reference station system designed to be located on a nearby platform or support boat will include a second GPS receiver and antenna, a UHF antenna and radio modem, and a personal computer with data collection and storage capacity. A trade-off must be performed between buoy positioning accuracy and receiver cost. The GPS receiver is currently the cost driver in buoy design, with dual-frequency survey receivers such as the Trimble SSE or Allen Osborne TurboRogue typically used. The dual-frequency capability permits high accuracy over large separations between the buoy and the ground reference stations. Several lower cost alternatives that will be considered include NovAtel's single-frequency high-performance C/A code and carrier receiver, a very low cost single-frequency C/A receiver such as the Rockwell Navcore V, and a dual-frequency codeless receiver to be designed based on an existing receiver built by AIR of Boulder, Colorado, which would track P(Y) code and L1/L2 carrier signals. We believe that the generic buoy and data collection and processing system would provide cost effective support for future scientific programs.

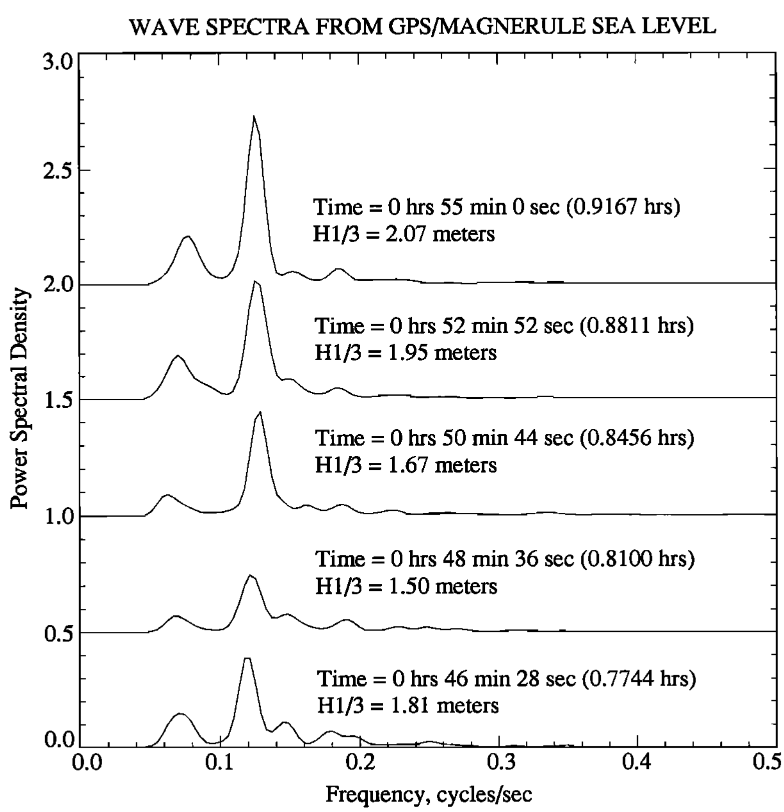

Figure 8. Wave spectra from the K&RS GPS/MagneRule sea level.

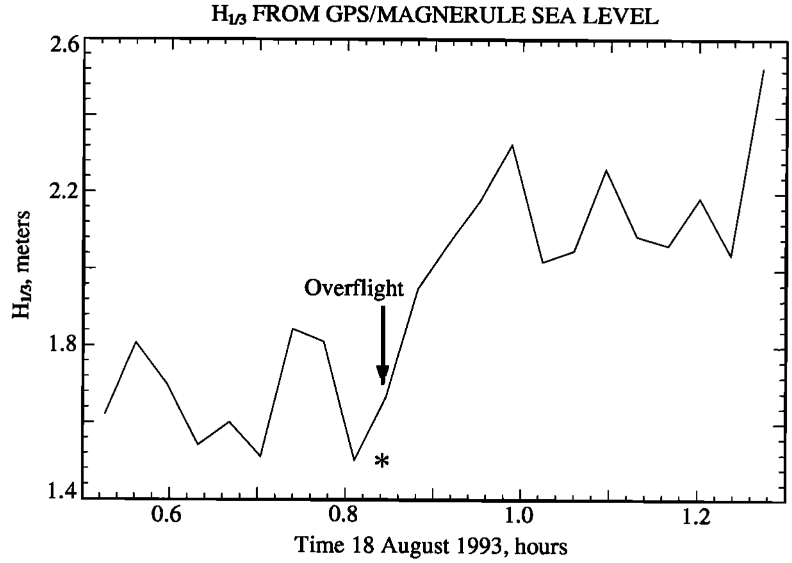

Figure 9. $H_{1/3}$ from the K&RS GPS/MagneRule sea level. $H_{1/3}$ from the TOPEX altimeter is indicated with an asterisk.

It should be noted that the altimeter bias estimated here is for a single altimeter pass. The error in the bias is composed of both random and systematic effects, so that when the buoy is deployed under multiple satellite passes the resulting error will be significantly smaller, perhaps less than 2 cm. Improved orbit determination in the future will result in a significant reduction in the single-pass error, thus also improving our ability to monitor the altimeter bias.

Conclusions

Based on the results presented here, and results obtained from previous deployments of a GPS-equipped buoy, it is concluded that such a buoy can be an effective tool for measuring and monitoring altimeter height biases. The buoy must be properly instrumented to provide waterline location and tilt information and a fiducial GPS site should be located within several hundred kilometers of the overflight point. The proximity of a fiducial GPS site is necessary so that differential GPS techniques can minimize atmospheric effects and GPS orbit error. As the length of this baseline increases, it becomes more difficult to estimate the initial position of the kinematic receiver and to correctly estimate phase bias parameters due to these errors. In the other extreme of a very short baseline (less than about 10 km), the two receivers will see essentially the same ionosphere. In these cases it is possible to process with L1 only data, which is less noisy than the ionosphere-corrected L3 data.

The Platform Harvest survey [*Gill et al.,* 1995] was performed under very difficult circumstances. The excellent agreement that we have found between the absolute GPS sea level and tide gauge measurements converted to absolute sea level not only confirms the validity of the GPS buoy approach but provides independent verification of the platform survey. We find it especially encouraging that GPS sea level obtained from two very different software packages had a mean difference of only 0.9 cm with a standard deviation of 1.2 cm over the length of the pass.

Acknowledgments. An experiment such as this requires the assistance of a number of people from different organizations. The authors thank Charles Morris and Steve DiNardo of the Jet Propulsion Laboratory for their assistance with platform operations and discussions, Bruce Haines of JPL for his help with closure analysis on the altimeter bias, Tom Kelecy of NAVSYS Corporation for helpful discussions on GPS solutions, Bob Leben of CCAR for providing information on the altimeter data, and Gerald Mader of NOAA who provided the K&RS software. We also acknowledge Texaco U. S. A. for the use of Platform Harvest and the staff of the platform for their advice and support. In particular we thank Richard Grunder, Gilbert Sotelo, Rick Moore, Hector Martinez, and Marcos Esqueda of VECO, Incorporated for their support at Platform Harvest during our experiment.

References

Bašić, T., and R. Rapp, Ocean wide reduction of gravity anomalies and SSH using Geos-3, Seasat, and Geosat altimetric data and ETOPOSU bathymetric data, *Rep. 416*, 89 pp., Dep. of Geod. Sci., Ohio State Univ., Columbus, 1992.

Bendat, J.S., and A.G. Piersol, *Random data: Analysis and Measurement Procedures*, 407 pp., Wiley-Interscience, New York, 1971.

Bertiger, et al., GPS precise tracking of TOPEX/POSEIDON: Results and implications, *J. Geophys. Res.*, this issue.

Christensen, E.J., et al., Calibration of TOPEX/POSEIDON at Platform Harvest, *J. Geophys. Res.*, this issue.

Gill, S.K., R.F. Edwing, D.F. Jones, T.N. Mero, M.A.K. Moss, M. Samant, H.H. Shih, and W.E. Stoney, NOAA/National Ocean Service Platform Harvest instrumentation, *Mar. Geod.*, *18*, in press, 1995.

International Earth Rotation Service, Annual Report for 1992, IERS Cent. Bur., Obs. de Paris, 1993.

Kelecy, T., G.H. Born, and C. Rocken, GPS buoy and pressure transducer results from the August 1990 Texaco Harvest Oil Platform Experiment, *Mar. Geod.*, *15*, 225-243, 1992.

Kelecy, T., M. E. Parke, G. H. Born and C. Rocken, Precise sea level measurements using the Global Positioning System, *J. Geophys. Res.*, *99*(C4), 7951-7959, 1994.

Lanyi, G.E., Tropospheric delay effects in radio interferometry, *JPL Prog. Rep. 42-78*, pp. 152-159, Jet Propuls. Lab., Pasadena, Calif., 1984.

Lichten, S.L., and J.S. Border, Strategies for high-precision Global Positioning System orbit determination, *J. Geophys. Res.*, *92*(B12), 12751-12762, 1987.

Mader, G.L., Dynamic positioning using Global Positioning System carrier phase measurements, *Manuscr. Geod.*, *11*, 272-277, 1986.

Morris, C.S., S.J. DiNardo, and E.J. Christensen, Overview of the TOPEX/POSEIDON Platform Harvest verification experiment, *Mar. Geod.*, *18*, in press, 1995.

Rocken, C., T. M. Kelecy, G. H. Born, L. E. Young, G. H. Purcell, and S. K. Wolf, Measuring precise sea level from a buoy using the Global Positioning System, *Geophys. Res. Lett.*, *17*(12), 2145-2148, 1990.

Schenewerk, M.S., J.R. MacKay, W. Kaff, M. Chin, and G.L. Mader, Rapid turnaround GPS ephemerides from the National Geodetic Survey, paper presented at ION GPS 93, Inst. of Nav., Salt Lake City, Utah, 22-24 Sept. 1993.

Tapley B.D., et al., Precision orbit determination for TOPEX/POSEIDON, *J. Geophys. Res.*, this issue.

P. Axelrad, G. H. Born, K. L. Gold, J. Johnson, K. W. Key, D. G. Kubitschek, and M. E. Parke, Colorado Center for Astrodynamics Research, Campus Box 431, University of Colorado, Boulder, CO 80309

E. J. Christensen, Jet Propulsion Laboratory, M/S 264-686, Pasadena, CA 91109

(Received November 19, 1993; revised April 4, 1994; accepted April 4, 1994.)